

Analysis of Pigments and Damages for the 19th Century White-Robed Water-Moon Avalokitesvara Painting in Gongju Magoksa Temple, Korea

Hye Ri Yang

Kongju National University

Chan Hee Lee (✉ chanlee@kongju.ac.kr)

Kongju National University

Jeongeun Yi

Kongju National University

Research Article

Keywords: Magoksa temple, White-Robed Water-moon Avalokitesvara Painting, Coloring technique, Traditional pigment, Synthetic composition

Posted Date: June 2nd, 2021

DOI: <https://doi.org/10.21203/rs.3.rs-559123/v1>

License: © ⓘ This work is licensed under a Creative Commons Attribution 4.0 International License. [Read Full License](#)

Abstract

The *White-Robed Water-Moon Avalokiteshvara* painting displayed on the rear wall of Daegwangbojeon (main hall) in Magoksa temple, is one of the representative Buddhist paintings in the late 19th century of Korea, and a valuable resource for understanding the coloring techniques and characteristics of Buddhist paintings in terms of expression and description in landscape painting. In this painting, the contours and colored surface remain undamaged, but blistering and exfoliation appear on some pigment layers. Furthermore, the partial decomposition of wooden materials due to wood-decay fungi and insect damage were found on the rear wall requiring proper treatment for long-term conservation. As the results of chromaticity and P-XRF analysis regarding the color pigment layer of the painting, the pigments were classified into ten types. The results suggest that the colors other than blue, green, yellow, red, black, and white were prepared by mixing two or more pigments. The types of pigments according to colors, were determined as traditional pigments with azurite; emerald green or clinoptilactite; massicot; minium or hematite; Chinese ink; and kaolin, white lead, and gypsum, respectively. Violet and pink colors were assumed to have been prepared by mixing white with blue and red. In most of these pigments, small amounts of synthetic compositions from the modern era were detected at many points.

1. Introduction

The *White-Robed Water-Moon Avalokiteshvara* is an artwork that represents the Buddhist paintings of Magoksa temple located on the rear wall on the west side of Daegwangbojeon (main hall), which is the dharma hall of Magoksa temple. A frame is made up of wood structures between high pillars, and several layers of mulberry fibers are applied to create a rear wall, which appears as if it were painted on a typical canvas. However, it is difficult to discover the exact date of creation because there is no manufacture date. In Magoksa temple, although this painting has been said to be painted by the Buddhist monk *māyā* Yakhyo (1846 to 1928), this claim is questionable because the expressions and descriptions of Amitabha about the crown of the white-robed *Gwaneum Bosal* (Buddhist Goddess of Mercy) are slightly different.

The lines are overall smooth, and the techniques of landscape paintings in the late Joseon Dynasty (17th to 19th century) of Korea can be seen in the expression of the rocks. Nevertheless, considering the formal description technique observed in the face of Buddha and the use of dark red, the creation period is estimated to be in the late 19th century. Although the contours and colored surface of this *White-Robed Water-Moon Avalokiteshvara* remain undamaged, there is blistering, exfoliation, and discoloration of some pigment layers; contamination and stains; cracks and separations of the pigment layers; and cracks and separations of the wall. Thus, the painting urgently requires stable conservation treatment.

This painting was safely dismantled after performing a basic investigation and emergency treatment at the site. It was then transferred in a vibration-free vehicle for precise conservation treatment, and it has recently been placed at its original location. Prior to the conservation treatment of the painting, this study recorded the degree and condition of the overall damage in detail and conducted a scientific investigation on the colored layer to analyze the components and characteristics of the pigments used for coloring. Through such research, we have studied the characteristics by analyzing colored pigments used in ancient Korean art works [1–4]. These results are important data that can reveal the pigments and coloring techniques used in Buddhist paintings at that time, which also can be used for research on long-term preservation and repair.

2. Object And Method

2.1. Object

This study was conducted prior to the conservation treatment of the *White-Robed Water-Moon Avalokiteshvara*, a Buddhist painting on the rear wall of main hall in Magoksa temple. It aimed to secure basic data that can be used for conservation treatment through the precise analysis of coloring pigments by each color. Thus the surface of the painting as well as the integrity and damage status of the pigment layer were reflected in a drawing, which was intended to be preserved as a record of the repair and treatment areas of the colored layer.

This *White-Robed Water-Moon Avalokiteshvara* painting is a colossal mural measuring 515cm in length and 296cm in width, with *Gwaneum Bosal* (Avalokiteshvara) in a white robe sitting on a lotus pedestal above a rippling wave and a strange rocky stone, with her left leg hanging down. She is at the center of the painting surface and facing the front in a half-lotus position, her right leg placed on her left (Fig. 1a). *Gwaneum Bosal* wears a white robe from her head to below knees and red bottoms having a green bottom with red hem and tied with a pink belt inside the white robe (Fig. 1a).

In addition, *Gwaneum Bosal* wears a crown on her head with a standing Amitabha statue in the middle to indicate identity as *Avalokiteshvara* (Figs. 1b and 1c). Her right hand rests comfortably on right leg, and her right ankle is held with left hand. Her hands and feet are large and realistically depicted (Fig. 1d). Behind *Gwaneum Bosal*, four bamboo trees are rising from the rough rocks on the left side (Fig. 1e); *Seonjae Dongja* (priestling) stands thereunder, leaning toward *Gwaneum Bosal* (Fig. 1f); and a *kundika*, in which a willow branch is arranged, is placed on the opposite rocks (Fig. 1g).

2.2. Method

In the preservation status investigations, the damage types of the colored layer were subdivided to create a map, and empirical data were presented to increase the reliability. This study applied a method with recently proven reliability in the damage assessment in the field of cultural heritage conservation science, including stone artifacts [5–6].

Damage map creation and non-destructive investigation for the painting as a research object were conducted with special care to prevent any impact on the painting by using an installed scaffold. First, the preservation status was precisely recorded by checking the damage status at the site, and the analysis target was further selected after selecting the colors, such as blue, green, yellow, red, black, and white, by visual observation to confirm the color status.

As the analysis point for each color, a site was selected, whose measurement area of approximately 5mm in diameter was sufficient among the colors in which the difference in color was distinguished by visual observation, and where the pigment in the base layer with the target color was not disturbed (Fig. 2). Non-destructive chromaticity and composition measurements were performed for the selected analysis points, and a trace amount of pigment that had flaked off was collected by using a sample for precision analysis. The names of the analysis points are indicated in Table 1.

Table 1
Summary on colors and designations for analysis points in this study.

Color	Blue		Green	Yellow		Red	Black	White	Violet	Pink
	Blue-1	Blue-2		Yellow-1	Yellow-2					
Mark	LBG	SB	BG	OY	Y	R	BL	W	V	P

In the detail investigation, chromaticity measurement, observation through a portable stereoscopic microscope, and elemental analysis through a portable X-ray fluorescence analyzer were performed. All were conducted through non-destructive analysis, and the same area was analyzed for each measurement item. Furthermore, the field analysis was carefully conducted by minimizing the applied pressure by selecting only the part of the color pigment that was most closely adhered onto the base layer to avoid any loss from the split colored layer due to the contact-based analysis.

A total of 55 analysis points were used to identify the components of the color pigments in this painting for measurement under classification into blue, green, yellow, red, black, and white series. This study secured quantitative data based on the results of a color component analysis that had already been reported for this study, and the types of pigments used in this painting were identified in comparison to the data on previously studied traditional pigments [7–14].

A CM-2500d spectrophotometer (KONICA MINOLTA) was used to measure the chromaticity of the pigments, and three measurements were obtained at the same point with a measurement area of 3 mm through the light source D65. The chromaticity values of the analyzed pigments were expressed by the CIELab system defined by the International Commission on Illumination (CIE), and the color coordinates were represented by luminosity (L^*), red to green value (a^*), and blue to yellow value (b^*). In addition, the color components can be more intuitively understood by indicating chromaticity (C^*_{ab}) and hue (h^*_{ab}) values on the polar coordinates. Chromaticity (Eq. 1) is expressed as a position between the center of the sphere (black) and the outer surface (white). Hue (Eq. 2) is expressed in angle, with red = 0°, yellow = 90°, green = 180°, and blue = 270° [15–16].

$$C^*_{ab} = (a^{*2} + b^{*2})^{1/2} \quad (1)$$

$$h_{ab} = \arctan(b^*/a^*) \quad (2)$$

The measurement range of L^* is from 0 to 100, and 100 refers to nearly white, which is close to white light, and 0 refers to black. The measurement range of a^* and b^* for the colorimeter used in this study is -100 to +100. The a^* indicates a redder color in a positive direction and a greener color in a negative direction; b^* indicates a yellower color in a positive direction and a bluer color in a negative direction.

In the component analysis for the color pigment at the site, an X-ray fluorescence spectrometer (P-XRF; Oxford Instruments, X-MET7500) was used for the part selected as the analysis location. The operating conditions of this spectrometer were an X-ray tube voltage of 15 to 40kV (40kV for heavy elements and 15kV for light elements) and a current of 10 to 50µA. Measurement was performed in the ore mineral mode, the analysis area was approximately 5mm in diameter, and the measurement time was 20 seconds each in conducting the elemental analysis on an atomic number of 15 or higher.

The name of each pigment, even with the same components, may vary depending on the period, region, material, supply route, particle size, and areas of use. This study mainly recorded the names used based on previous studies regarding the color pigments of paintings. Furthermore, the estimation of black pigments and raw materials was performed through a comprehensive review of the results of scanning electron microscope-energy dispersive spectroscopy (SEM-EDS) analysis and X-ray fluorescence analysis performed in the field investigation by collecting a trace amount of color pigment samples that had flaked off during the stripping process.

3. Results And Interpretation

3.1. Preservation Status

The types of damage observed on the painting surface of *White-Robed Water-Moon Avalokiteshvara* are typically divided into microcracks (Fig. 3a), separation (Fig. 3b), fragmentation (Fig. 3c), contamination (Fig. 3d), and blistering and exfoliation of the pigment layer (Figs. 3e and 3f). Overall, although the contour lines and colored surfaces of this painting remain undamaged, damage appears on the painting surface along with blistering and exfoliation of some pigment layers, cracks and separation of the pigment layer, and cracks and separation of the wall (Fig. 3).

The blistering and exfoliation of the pigment layer are mainly observed around the face and on the red bottoms of the *Gwaneum Bosal*, which is believed to be accompanied by contraction, expansion, and cracking due to moisture. Moreover, after completely stripping the painting, the preservation condition of the wood materials on the rear wall were checked. As a result, it was found that the deterioration of the front lining paper and the wooden frame had severely progressed due to decomposition by wood-decay fungi and insect damage (Figs. 3g and 3h).

The structural condition of the wooden frame constituting the painting wall was found to be relatively stable, and while there were cracks and separation along the edge of the wall, the preservation condition of the mural painting as a whole was fair. In addition, because the blistering, exfoliation of the colored

layer, contamination, and fragmentation were found to be scattered throughout the painting surface, it was recommended that appropriate measures for long-term preservation be taken.

3.2. Chromaticity Measurements

The pigments used to color this painting mainly include blue, green, yellow, red, black, and white, and violet and pink appear in smaller amounts (Fig. 4). This study measured the chromaticity of a total of 55 points for representative color pigments: six points for blue, eleven points for green, seven points for yellow, eight points for red, six points for black, eleven points for white, and ten points for other colors (Fig. 5 and Table 2).

Table 2
Descriptive values statistics (mean, standard deviation, maximum and minimum) for the CIELab colour parameters of the painting in this study.

		L*	a*	b*	C* _{ab}	h _{ab}			L*	a*	b*	C* _{ab}	h _{ab}	
BLU E	1	Mean	65.56	-1.29	11.56	65.56	96.15	R	Mean	39.92	20.72	17.04	39.92	40.10
		SD	0.08	0.69	1.85	0.69	2.38	E	SD	3.80	5.02	2.37	5.02	8.17
		Max	65.62	-0.80	12.87	12.87	97.83	D	Max	46.22	30.39	19.68	19.68	52.34
		Min	65.50	-1.77	10.25	10.28	94.46		Min	32.96	12.71	12.45	20.80	29.07
	2	Mean	70.71	-5.08	10.52	70.71	116.09	B	Mean	34.52	1.81	6.59	34.52	79.22
		SD	2.39	0.97	1.49	0.97	6.68	L	SD	12.92	3.50	9.54	3.50	4.84
		Max	72.89	-3.73	12.17	12.17	122.15	A	Max	58.65	8.95	25.86	25.86	85.80
		Min	68.06	-6.04	8.96	10.46	108.21	C K	Min	25.42	0.25	1.27	1.29	70.91
G R E E N	Mean	48.01	-10.17	4.12	48.01	156.76	W	Mean	73.35	0.84	15.78	73.35	87.85	
	SD	5.08	3.88	3.36	3.88	15.76	H	SD	8.48	1.64	4.43	1.64	6.21	
	Max	56.50	-3.87	11.75	11.75	184.27	I	Max	80.72	2.66	21.78	21.78	101.85	
	Min	42.18	-15.70	-1.10	5.80	128.82	T E	Min	53.87	-2.55	8.36	8.36	82.34	
Y E L L O W	1	Mean	57.41	10.68	26.40	57.41	67.90	V	Mean	52.35	-0.57	-1.24	52.35	61.20
		SD	3.19	0.99	2.93	0.99	1.95	I O	SD	1.32	0.18	0.71	0.18	20.66
		Max	60.56	11.75	28.75	28.75	69.50	L	Max	53.28	-0.44	-0.74	-0.74	75.81
		Min	54.53	9.36	22.62	24.48	65.30	E T	Min	51.42	-0.70	-1.74	1.02	46.59
	2	Mean	59.41	3.38	30.54	59.41	83.94	P	Mean	64.87	9.26	13.80	64.87	53.42
		SD	2.41	2.65	5.70	2.65	4.33	I	SD	2.43	5.67	3.33	5.67	9.14
		Max	61.02	5.75	37.08	37.08	88.93	N	Max	68.42	17.21	18.43	18.43	59.88
		Min	56.64	0.52	26.61	26.89	81.19	K	Min	62.92	3.91	10.65	13.76	46.96

SD; standard deviation

The chromaticity values for all measurement points represent various luminosity values, which are distributed between red to yellow (h_{ab} : 0 to 90°) and yellow to green (h_{ab} : -90 to 0°) as a result of projection on the CIE Lab quadrant. Among the values, yellow and red pigments have relatively higher chromaticity and hue variability than blue and green pigments (Table 2, Fig. 5).

Regarding the chromaticity range of the blue-1 pigment, L*, a*, and b* range from 65.5 to 65.62 (mean 65.56), -1.77 to -0.8 (mean -1.285), and 10.25 to 12.87 (mean 11.56), respectively. Regarding the chromaticity of the blue-2 pigment, L* on means is 70.71, a* is -5.07, and b* is 10.52, respectively. Blueness increases as b* increases in the negative direction, while the measured blue-2 pigments all have positive b* values, showing that the blueness of the blue-2 pigments is lower than that of the blue-1 pigments (Table 2 and Fig. 5).

According to the result of measuring the chromaticity for the green pigments, L*, a*, and b* range from 42.18 to 54.82 (mean 48.00), -15.7 to -3.87 (mean -10.16), and -3.75 to 6.57 (mean 2.71), respectively. As a* increases in the negative direction, greenness increases, and the a* values of all analysis points are negative. BG-7 shows the highest green level with a L* of 53.88, a* of -15.7, and b* of 11.75, and BG-10 shows the lowest green level with a L* of 44.14, a* of -3.87, and b* of 4.81 (Table 2 and Fig. 5).

Regarding the chromaticity of the yellow-1 pigments, L*, a*, and b* range from 54.53 to 60.56 (mean 57.41), 9.36 to 11.75 (mean 10.67), and 22.62 to 28.75 (mean 26.39), respectively. In the case of the yellow-2 pigments, L*, a*, and b* range from 56.64 to 61.02 (mean 57.41), 0.52 to 5.75 (mean 3.38), and 26.61 to 37.08 (mean 30.54), respectively. Yellowness increases as b* increases in the positive direction. Y-3 shows the highest yellowness, and OY-3 shows the lowest yellowness (Table 2 and Fig. 5).

The chromaticity of red pigments is widely distributed in the + a* and + b* coordinate planes. L*, a*, and b* range from 32.96 to 62.22 (mean 39.92), 12.71 to 30.39 (mean 20.67), and 14.45 to 19.68 (mean 17.28), respectively. Redness increases as a* increases in the positive direction. R-2 shows the highest redness with a L* of 38.38, a* of 30.39, and b* of 17.43, and R-8 shows the lowest redness with a L* of 46.22, a* of 12.71, and b* of 16.47 (Table 2 and Fig. 5).

The chromaticity range of black pigments is concentrated near the origin. L*, a*, and b* range from 25.42 to 58.65 (mean 34.51), 0.25 to 8.95 (mean 1.80), and 1.27 to 25.9 (mean 6.59), respectively. The analysis point closest to the origin is BL-1, where L* is 25.43, a* is 0.25, and b* is 1.27. The chromaticity range of white pigments is distributed vertically along the + b* axis. L*, a*, and b* range from 53.87 to 80.72 (mean 73.99), -2.55 to 2.89 (mean 1.02), and 8.36 to 21.78 (mean 16.09), respectively. The analysis point with the lightest color corresponds to W-8, and the analysis point with the darkest color corresponds to W-9 (Table 2 and Fig. 5).

Meanwhile, regarding the chromaticity range of violet pigments, L*, a*, and b* range from 51.42 to 53.28 (mean 52.35), -0.74 to -0.44 (mean -0.57), and -1.74 to 0.74 (mean -1.24), respectively. Because a* and b* show negative values at both measurement points, the redness and yellowness are not high, which does not deviate significantly from the negative direction. Furthermore, regarding the chromaticity range of pink pigments, P-1 shows higher redness and yellowness than P-4 (Table 2 and Fig. 5).

3.3. Chemical Compositions by P-XRF

P-XRF was utilized to analyze the chemical composition of pigments in *White-Robed Water-Moon Avalokiteshvara* painting. The analysis locations were the same as the points for the chromaticity measurement and observation using the stereoscopic microscope. The analysis location for each colored pigment is shown in Fig. 4.

In analyzing a pigment layer through P-XRF, it is difficult to accurately measure only the pigment compositions because X-rays penetrate through the thin pigment layer and further analyze the underlying background. To overcome these shortcomings, studies have aimed to unravel only the components of the pigment from which the background component was removed. This study also detected the compositions of the pigment layer according to the method provided by Lee *et al.* (2012), Jeon *et al.* (2009), and Jeon and Lee (2011) [1–3].

Two types of blue pigments were used for the basic coloring of this painting. According to the results of chromaticity measurement and observation using the stereoscopic microscope, an analysis was conducted by classifying the results into Blue-1 and Blue-2. If grayish blue ((Co,Ni)As₂) is used as a blue pigment, cobalt and nickel compositions are detected. However, these were not detected in this painting. On average, 9,037 ppm (6,363 to 11,710 ppm) and 33,763 ppm (12,844 to 59,991 ppm) of Cu were detected in Blue-1 and Blue-2 analysis points, respectively.

Thus, the results suggest that the color depth was raised by mixing a white pigment with azurite (Cu₃(CO₃)₂(OH)₂), which is one of the traditional blue pigments. The detection of the high concentration of Ca, Pb, and S compositions at all analysis points further suggests that the color shade could have been adjusted by oyster shell white (CaCO₃) or white lead (2PbCO₃·Pb(OH)₂) (Table 3 and Fig. 6).

Table 3
 Representative concentrations (ppm) by P-XRF of pigments on the studied painting. Numbers are the same as those of Fig. 2. Abbreviations as in Table 1.

No.		Si	Al	Fe	Ti	Ca	Mg	K	S	Cl	As	Ba	Cu	Hg
Blue-1	Mean	188,019	69,928	18,726	1,134	214,938	ND	8,426	55,078	ND	4,285	ND	9,037	ND
	SD	39,246	23,248	18,419	158	98,813	ND	11,915	17,751	ND	2,270	ND	3,781	ND
	Max	215,770	86,366	31,750	1,246	284,809	ND	16,851	67,630	ND	5,890	ND	11,710	ND
	Min	160,268	53,489	5,702	1,022	145,067	ND	ND	42,526	ND	2,680	ND	6,363	ND
Blue-2	Mean	119,355	50,436	9,147	1,121	341,514	ND	1,359	57,663	ND	4,228	ND	33,763	ND
	SD	2,029	4,718	4,888	149	30,790	ND	2,717	14,518	ND	309	ND	24,317	ND
	Max	121,166	56,648	14,074	1,265	368,397	ND	5,434	78,262	ND	4,616	ND	59,991	ND
	Min	117,417	45,759	4,783	930	307,801	ND	ND	45,364	ND	3,880	ND	12,844	ND
Green	Mean	115,166	42,613	25,780	766	35,175	30,524	23,684	28,938	24,820	110,568	ND	149,915	46
	SD	73632	21629	23358	623	50422	32902	20590	12510	14286	76859	ND	94787	153
	Max	261,796	72,956	80,064	1,947	148,206	80,061	67,626	49,617	47,419	296,732	ND	311,848	507
	Min	54,172	ND	7,202	ND	3,609	ND	6,208	11,315	ND	13,716	ND	13,321	ND
Yellow-1	Mean	66,816	ND	7,555	ND	11,017	ND	1,782	90,707	ND	ND	55,919	8,756	548
	SD	8,041	2,975	1,902	11,116	7,225	ND	3,564	34,826	4,720	ND	12,828	5,766	866
	Max	77,951	19,286	9,885	81,718	17,343	ND	7,128	132,885	30,303	ND	74,749	14,337	1,82
	Min	58,842	12,453	5,526	58,638	4,424	ND	0	59,470	19,529	ND	46,032	3,510	ND
Yellow-2	Mean	60,278	14,611	12,199	72,400	3,727	ND	5,764	140,291	29,398	2,005	67,742	6,389	ND
	SD	7,837	3,079	4,394	18,502	1,900	ND	4,992	9,996	6,403	3,472	13,465	398	ND
	Max	68,560	17,255	15,254	83,346	5,877	ND	8,684	151,754	36,457	6,014	82,836	6,707	ND
	Min	52,979	11,230	7,164	51,038	2,277	ND	0	133,392	23,966	ND	56,966	5,943	ND
No.	Si	Al	Fe	Ti	Ca	Mg	K	S	Cl	As	Ba	Cu	Hg	
Red	Mean	109,215	51,483	56,471	17,933	30,023	ND	11,647	126,608	27,071	241	20,687	4,008	5,52
	SD	67,900	51,070	47,584	20,026	28,673	ND	3,936	47,290	25,416	462	24,411	2,008	7,66
	Max	208,888	141,941	144,556	56,922	65,373	ND	16,945	176,624	59,990	1,184	66,173	7,032	16,2
	Min	30,988	8,371	13,311	943	2,229	ND	6,850	42,744	ND	ND	ND	1,765	ND
Black	Mean	196,408	81,706	28,058	1,976	85,953	ND	33,818	71,263	19,528	1,054	0	3,348	ND
	SD	76,697	39,621	14,544	507	75,135	ND	17,405	41,787	30,856	1,342	0	2,565	ND
	Max	252,724	122,297	46,489	2,514	194,497	ND	55,483	125,777	68,180	3,000	0	7,576	ND
	Min	63,842	16,992	11,076	1,098	16,859	ND	12,746	35,642	ND	ND	ND	678	ND
White	Mean	151,220	42,596	13,109	4,440	225,922	39,842	7,623	47,701	3,594	803	7,159	2,140	ND
	SD	69,768	29,725	8,795	3,905	70,754	69,479	8,007	23,056	11,918	1,003	12,349	2,351	ND
	Max	244,566	89,153	27,255	11,088	341,179	175,919	24,628	98,436	39,529	2,952	28,798	7,406	ND
	Min	58,740	ND	4,361	1,039	95,963	ND	ND	ND	ND	ND	ND	559	ND
Violet	Mean	234,391	51,155	26,454	917	34,920	73,223	21,793	72,511	ND	442	0	27,799	ND
	SD	13,900	3,374	4,524	130	3,895	2,331	3,268	8,832	ND	624	0	7,828	ND
	Max	244,220	53,541	29,653	1,009	37,674	74,871	24,104	78,756	ND	883	0	33,334	ND
	Min	224,562	48,769	23,255	825	32,165	71,575	19,482	66,265	ND	0	0	22,263	ND
Pink	Mean	177,186	20,127	11,374	8,137	109,155	96,045	8,041	33,532	4,188	150	10,220	5,786	ND
	SD	89,135	13,519	4,724	4,925	130,723	67,834	5,850	29,904	8,377	300	8,607	6,068	ND
	Max	230,166	28,167	16,438	13,734	304,902	158,080	13,997	71,002	16,753	599	20,948	13,953	ND
	Min	43,800	ND	7,037	1,758	34,669	ND	ND	ND	ND	ND	ND	1,115	ND

No.	Si	Al	Fe	Ti	Ca	Mg	K	S	Cl	As	Ba	Cu	Hg
ND; not detected													

According to the results of the P-XRF analysis regarding the green pigment layer measured at a total of 11 points, the major compositions detected were elements such as S, Ca, Ti, Fe, Cu, As, and Pb. However, the average content of Cu and As showed a significant difference: 149,915 ppm (13,321 to 311,848 ppm) and 110,568 ppm (13,716 to 296,732 ppm). Typically, when Cu and As are simultaneously detected in the composition of a green pigment, it is considered emerald green ($\text{Cu}(\text{C}_2\text{H}_3\text{O}_2)_2 \cdot 3\text{Cu}(\text{AsO}_2)_2$). However, in the relative content ratios of emerald green, the content of As is much higher than that of Cu. Although a high As content was detected in the green pigment used in this painting, it was difficult to determine it as emerald green because the ratio of As was mostly lower than that of Cu (Table 3 and Fig. 6).

The difference in the Cu and As content at each analysis point may have been affected by the thickness of the overlapped color. Furthermore, the pigments used for the face of Buddha and *Keyura* accessories remained relatively undamaged, whereas those used on the feet and the lower parts fell off, resulting in a relatively small amount. Thus, these results suggest that clinoatacamite ($\text{Cu}_2(\text{OH})_3\text{Cl}$) made up of copper-based raw materials was mainly used for the green pigment layer, and it was likely painted over by modern pigments given the result that the Ca and Cl content is relatively high at some points (Table 3 and Fig. 6).

The points classified as yellow were analyzed by dividing them into Yellow-1 and Yellow-2 according to the results of chromaticity measurement and observation using the stereoscopic microscope. Among the main constituent elements detected, Al and Si appear to have been simultaneously detected as a dead color paint component using a white pigment, such as *ūrnā* (Table 3). The content of Pb was the highest at all points with an average of 288,094 ppm (246,801 to 323,689 ppm) and 252,850 ppm (187,988 to 289,484 ppm), in Yellow-1 and Yellow-2, respectively, followed by S with an average of 90,707 ppm (59,470 to 132,885 ppm) and 140,291 ppm (133,392 to 151,7544) (Table 3 and Fig. 6). Thus, the color yellow can be assumed to lower the chromaticity by mixing white pigments with massicot.

However, the detection of As (6,014 ppm) only in Y-1 suggests that orpiment (As_2S_3) and massicot (PbO) were mixed with a white pigment for coloring. Regarding the white pigment used in the color combination, the Ti content was relatively high at 72,827 ppm (58,638 to 81,718 ppm) and 72,400 ppm (51,038 to 83,346 ppm) in Yellow-1 and Yellow-2, respectively, which can be assumed to be titanium dioxide (TiO_2). In addition, compared to other color pigments, Ba is highly likely to be a modern pigment due to the detection of high levels of Ba with an average of 55,919 ppm (46,032 to 74,7499 ppm) and 67,742 ppm (56,966 to 82,836 ppm) in Yellow-1 and Yellow-2, respectively (Table 3 and Fig. 6).

According to the results of the component analysis on red pigments, the main composition were Pb, S, and Hg, and Si and Al were detected at all measured points. It can be assumed that the colored white clay under the red layer was detected together with the pigments. According to the results of the P-XRF analysis regarding a total of eight points, the patterns of constituent elements were classified into two, depending on the presence and content of Fe, Pb, and Hg.

Points R-1 to R-4 show a high Pb content with an average of 366,476 ppm (360,982 to 373,432 ppm). Points R-5 to R-8 show a relatively high content of Fe, with an average of 94,592 ppm (63,070 to 144,556 ppm). Thus, the red colors appear to be a mixture of minium (Pb_3O_4) or minium and hematite (Fe_2O_3), and it can be assumed that cinnabar (HgS) was used in smaller amounts together with these (Table 3 and Fig. 6).

According to the analysis results regarding the black layer, elements such as P, Fe, K, S, Ca, Ti, Cl, and Cu were detected. Most of these elements are not components of black pigments, which suggests the effect of dead color paints. However, no element indicating black color was detected (Table 3 and Fig. 6). The traditional black pigment is an Chinese ink, which is a carbon compound. Because Chinese ink is composed of light elements, it is difficult to detect with P-XRF. Thus, because only the same components as the white pigment used in the base layer were mainly detected at the measurement point of the black pigment, Chinese ink was likely used for black color development, requiring additional review.

In this black layer, the detection of slightly high levels of Pb and Ca, with an average of 59,164 ppm (0 to 331,475 ppm) and 85,953 ppm (from 16,859 to 194,497 ppm) through P-XRF, suggests that white lead and oyster shell white were mixed to lower the concentration of black pigment. Among the analysis points, the highest detection of Pb at 331,475 ppm in the right pupil of the *Gwaneum Bosal* statue suggests that the pigment was reapplied several times (Table 3 and Fig. 6).

The white color is mainly used on the *Gwaneum Bosal* statue and cloth, in which elements such as Si, K, and Al were detected through the P-XRF analysis. Among these elements, the average contents of Si, K, and Al were 151,220 ppm (58,740 to 244,566 ppm), 11,979 ppm (5,722 to 24,628 ppm), and 46,856 ppm (7,846 to 89,153 ppm), respectively, and these high levels suggest the high likelihood of the use of kaolin ($\text{Al}_2\text{Si}_2\text{O}_5(\text{OH})_4$). The detection of Ca and S with an average of 225,922 ppm (95,963 to 341,179 ppm) and 52,471 ppm (36,456 to 98,436 ppm) suggests that gypsum was likely mixed with feldspathic kaolin (Table 3 and Fig. 6).

The color violet was mainly used for coloring the *daeui* part of *Gwaneum Bosal*. According to the result of the P-XRF analysis, Cu and Fe were detected with an average of 27,799 ppm (22,263 to 33,334 ppm) and 26,454 ppm (23,255 to 29,653 ppm), respectively, as the main compositions. Because the composition is similar to that of the blue pigment, and high levels of Fe and Pb are detected, the mixture of azurite, hematite, and minium can be assumed (Table 3 and Fig. 6).

In addition, Ca, S, and Mg were detected here at 34,920 ppm (32,165 to 37,674 ppm), 72,511 ppm (66,265 to 78,756 ppm), and 72,223 ppm (71,575 to 74,871 ppm), respectively. This result suggests the addition of gypsum or talc ($\text{Mg}_3\text{Si}_4\text{O}_{10}(\text{OH})_2$), which is a white pigment, or the detection of constituent minerals in

the base layer to lower the chromaticity (Table 3 and Fig. 6).

The color pink is painted on the chest top part of *Gwaneum Bosal* as well as the ears of Buddha. According to the results of the P-XRF analysis, Si, Mg, Ca, and S were detected with an average of 177,186 ppm (43,800 to 230,1666), 128,059 ppm (104,302 to 158,080 ppm), 109,155 ppm (34,669 to 304,902 ppm), and 44,710 ppm (23,002 to 71,002 ppm), respectively. This result becomes the basis for assuming the use of kaolin or talc as a white pigment in combination with pink. Moreover, the detection of high levels of Pb and Fe with an average of 99,309 ppm (2,228 to 277,324 ppm) and 11,374 ppm (7,0378 to 16,438 ppm) suggests that the color depth was raised by mixing kaolin or talc with minium and hematite in terms of components (Table 3 and Fig. 6).

4. Sem-eds Analysis

Although the locations of the micro-fragments of the flaked-off pigments collected during the stripping process for the repair of the *Gwaneum Bosal* were not clearly identified on this painting, a pale blue pigment was found underneath the thin black layer. Based on this finding, the colored layer was closely observed on a SEM (TESCAN, MIRA3), and the constituent elements on the pigment layer were analyzed using an EDS (Bruker, Quantax 200) mounted onto the SEM (Fig. 7).

According to the observation at high magnification with the SEM, the microtextures of the pigment layer can be divided into two layers: a black layer and a cyan layer (Fig. 7c). The elemental mapping regarding the black pigment part confirmed that carbon was more distributed in the black part than in the light cyan part (Fig. 7e). An observation at 3,000 magnification of this part showed that carbon particles with a diameter of 5nm were relatively uniformly coated on the smooth surface (Fig. 7f).

According to the results of the EDS analysis regarding this matter, a significantly high carbon (C) content was detected with an average of 60.30 wt.% (Table 4). In particular, no compositions other than the base layer components underneath the black color were detected, suggesting that Chinese ink, which is composed mainly of carbon, was used for coloring (Figs. 7c to 7g, and Table 4). Furthermore, although the SEM analysis regarding the pigments attached to the background paper showed a large number of Blue-1 pigment particles that had exfoliated onto the tissue composed of mulberry fibers, no specific components were detected (Figs. 7b and 7h).

Table 4
Results of SEM-EDS analysis (wt.%) on samples after exfoliation from the painting in this study. The measuring points are shown in Fig. 7.

No.	Si	Al	Fe	Ca	Mg	Na	K	C	O
1	14.62	8.24	0.62	-	0.91	1.32	2.51	24.81	46.97
2	6.01	3.39	0.65	0.3	0.88	0.55	1.09	67.42	19.71
3	3.83	4.37	0.74	1.41	9.12	-	1.05	54.36	25.12
4	15.7	4.34	1.63	-	5.9	0.18	2.25	22.64	47.36
5	6.62	3.51	1.45	0.89	7.67	-	1.41	49.65	28.8
6	3.84	4.14	0.71	1.42	9.15	-	1.12	54.33	25.29
7	1.26	1.46	0.7	1.36	-	-	0.85	85.57	8.8
8	1.43	0.88	1.24	0.63	0.24	-	0.87	88.12	6.59

5. Discussions

This study secured basic data on the types, compositions, raw materials, and colors of the pigments used in this painting through a scientific investigation and precise analysis of *White-Robed Water-Moon Avalokiteshvara* of main hall in Magoksa temple and the pigments remaining on the wooden frame after its stripping. The Korean National Research Institute of Cultural Heritage has reported on traditional pigments and color-developing elements based on analysis of various periods and cultural heritages.

Based on this data, in reviewing the analysis results regarding the target of this study, small amounts of modern synthetic pigments were identified at many points. Table 5 shows the results of the analysis using P-XRF and SEM-EDS, which are classified into the color series of pigments according to major color-developing elements.

Table 5
Summary on detected elements and estimated pigments for the painting in this study.

Color	Major Elements	Minor Elements	Interpreted Pigments
Blue-1	Cu	Fe, Ti, Ca, Mg, Na, K, S, Cl, As, Pb, Zn	Azurite + Lead White or White Clay
Blue-2		Fe, Ti, Ca, Mg, K, S, Cl, As, Pb	
Green	Cu, Cl	Fe, Ti, Ca, Mg, K, S, As, Co, Pb	Emerald Green, Clinoatacamite
Yellow-1	Pb, S	Fe, Ti, Ca, Mg, K, Cl, As, Ba, Cu, Hg	Litharge on Lead White
Yellow-2		Fe, Ti, Ca, Mg, K, Cl, As, Ba, Cu	
Red	Fe, Pb, Hg, S	Ti, Ca, K, Cl, Ba, Cu	Hematite, Red Lead (or Cinnabar)
Black	C	Fe, Ti, Ca, Mg, K, S, Cl, As, Cu, Pb, Zn	Chinese Ink
White	Al, Si, Pb	Mg, P, S, Ca, Ti, Mn, Fe, Cu, Zn, As, Ba	Lead White and White Clay
Violet	Cu, Fe, Pb	Ti, Ca, Mg, Mn, K, S, As, Zn	Azurite + Hematite + Lead White
Pink	Ca, Pb	Fe, Ti, Mg, K, As, Cu	Red Lead and Oyster Shell W.

Two types of blue pigments were assumed to be used for raising the color depth by mixing a white pigment with azurite ($\text{Cu}_3(\text{CO}_3)_2(\text{OH})_2$). Regarding the average chromaticity, L^* , a^* , and b^* are 11.6, 65.6, and -1.3, respectively, for Blue-1 pigment and 70.7, -5.1, and 10.5 for Blue-2. The higher L^* value for Blue-2 suggests that Blue-2 was mixed with a larger amount of white pigment to lower the chromaticity. The white pigment used in this case is assumed to be white lead, kaolin, or titanium dioxide (Table 5).

As pigments that are color development sources for green, copper chloride-based emerald green and clinoatacamite were identified, and white pigments such as white lead and kaolin were used as auxiliary materials for color combination, depending on the coloring position. The average chromaticity of the green series was determined as a L^* of 48.0, a^* of -10.2, and b^* of 4.1, and the chromaticity varied slightly depending on each analysis point.

Orpiment and massicot were identified as yellow pigments. These two types of yellow colors were mixed with white pigments to adjust their chromaticity for color combination. S and Pb were highly detected at most of the measurement points, suggesting that massicot (PbO) was likely used in combination with white lead or gypsum.

A trace amount of As was detected at the Yellow-2 point, which was difficult to determine as orpiment (As_2S_3) because the pigments colored on the background may have been analyzed together with it. The average chromaticity of Yellow-1 was determined as a L^* of 57.4, a^* of 10.7, and b^* of 26.4, and that of Yellow-2 was determined as a L^* of 59.4, a^* of 3.4, and b^* of 30.5. Thus, Yellow-1 was higher in luminosity, while Yellow-2 was higher in yellowness.

The compositions of Fe, Pb, S, and Hg were detected as color development sources for red pigments, which have compositions of hematite, cinnabar, and minium in common. This result suggests a mixture of hematite and minium as well as white pigments, such as lead and kaolin, for color combination. Among these analysis points, 56,922 ppm of Ti was detected in R-2, which suggests that titanium dioxide was likely used. The average chromaticity of red pigments including various color ranges was determined as a L^* of 39.9, a^* of 20.7, and b^* of 17.0, showing a tendency of low chromaticity and redness, and there was no significant difference in the average values of chromaticity for each measurement point.

The black pigments were all assumed to be amorphous Chinese ink. The average chromaticity of the black series was determined as a L^* of 59.4, a^* of 3.4, and b^* of 30.5, showing no significant difference at most of the analysis points, whereas the black pigment used for coloring the bamboo in the top right corner of *Gwaneum Bosal* showed the highest values with a L^* of 49.92, a^* of -10.91, and b^* of 1.75.

Kaolin and white lead were identified as pigments that become color development sources for the color white. Kaolin is composed of various minerals, which are subdivided into kaolinite with feldspar, and mica. The results suggest that white pigments were used alone, mixed with pigments of other colors, or used as extenders. The average chromaticity of the white pigments was determined as a L^* of 74.0, a^* of 1.0, and b^* of 16.1.

Violet and pink were used as auxiliary colors for coloring this painting. The analysis results of pigments showed that their composition was similar to that of the blue pigments, and the detection of Fe and Pb indicated that white lead was mixed with azurite or hematite. The average chromaticity of the color violet was determined as a L^* of 52.4, a^* of -0.6, and b^* of -1.2, which has lower chromaticity and higher blueness than the blue pigments.

The pink pigments were estimated to be a mixture of minium and oyster shell white due to the detection of high levels of Ca and Pb at almost all measurement points. Furthermore, the results suggested that Mg, Al, and Fe were detected at the measurement points of P-2 to P-4 due to the influence of the base layer. The average chromaticity of the pink pigments was determined as a L^* of 63.7, a^* of 11.0, and b^* of 13.8, which shows high luminosity and slight reddishness.

Elements such as Ti, Ba, and Hg were identified in most points on this painting, and thus, it was impossible to rule out the possibility that industrial synthetic pigments were used in the repair process. Further research is required, such as more accurate component analysis and identification for each color of the pigment, to confirm the traditional pigments that were used prior to modern synthetic pigments. Table 5 summarizes the analysis results and estimated pigments for the aforementioned ten types of pigments.

Amorphous carbon was observed in the black pigment remaining on the wooden frame after this painting was stripped. Although P, S, and Pb were also detected, this was assumed to be due to interference from the contaminants and the surrounding pigments. In addition, green, white, grayish white, and red pigments appeared, and the element content ratio of each color pigment was highly similar to that of this painting. Thus, the pigments remaining on the wooden frame are assumed to have been influenced by the pigments used in this painting.

6. Conclusions

1. The *White-Robed Water-Moon Avalokiteshvara* painting displayed on the rear wall of main hall in Magoksa temple, is painting representative of Buddhist paintings in the late 19th century of Korea, and a valuable resource for understanding the coloring techniques and characteristics of Buddhist paintings in terms of expression and description methods in landscape painting.
2. In this painting, the contours and colored surface remain undamaged, but blistering and exfoliation appear on some pigment layers, and fragmentation and microcracks are found along with cracks and separation of the wall. In addition, the surface is contaminated by scattered dust and animal excrement, also showing a partial loss.
3. The exfoliation and damage of the color pigment layer are severe around the face of Buddha and the red bottoms in *Water-Moon Avalokiteshvara*. Furthermore, the partial decomposition of wooden frame due to wood-decay fungi and insect damage were found on the rear wall that was exposed after the painting was stripped, requiring proper treatment for long-term conservation.
4. As the results of chromaticity and P-XRF analysis regarding the color pigment layer of this painting, the pigments were classified into ten types. The results suggest that the colors other than blue, green, yellow, red, black, and white were prepared by mixing two or more pigments.
5. The types of pigments according to color, blue, green, yellow, red, black, and white were determined as azurite; emerald green or clinoatacamite; massicot; minium or hematite; Chinese ink; and kaolin, white lead, and gypsum, respectively. Violet and pink colors were assumed to have been prepared by mixing white with blue and red.
6. The analysis result of the wooden frame's pigments showed the similarity to the painting in terms of color pigments. However, it was difficult to accurately identify the compositions of the remaining pigments in the process of stripping this painting, because the thickness of the colored layer decreased significantly, and interference between contaminants and surrounding pigments occurred.
7. In most of these pigments, small amounts of synthetic pigment components from the modern era were detected at many points. In addition, a detailed further examination of the cross-section of the pigment layer is required because of the overlap between the traditional pigments and the modern pigments that were used for repair.

Abbreviations

LBG: Blue-1; SB: Blue-2; BG: Green; OY: Yellow-1; Y: Yellow-2; R: Red; BL: Black; W: White; V: Violet; P: Pink

Declarations

Acknowledgements

Not applicable.

Author's contributions

All authors contributed to the planning, design of this article, performed the data acquisition and data analysis, and HRY, JY and CHL wrote the manuscript and all authors revised it critically. All authors read and approved the final manuscript.

Funding

Not applicable.

Availability of data and materials

Not applicable.

Competing interests

The authors declare that they have no competing interests.

Author details

Department of Cultural Heritage Conservation Sciences, College of Natural Sciences, Kongju National University, Gongju, 32588, Republic of Korea.

References

1. Lee CH, Lee JE, Han NR. Characterization and analysis of painted pigments for the clay statues in Donggwanwangmyo Shrine, Seoul. *Journal of Conservation Science*. 2012;28;101-112.

2. Jeon YG, Kim WK, Jo YH, Han DR, Kim SD, Lee CH. Pigment analysis and nondestructive deterioration diagnosis of the wall paintings in Gwanyongsayaksajeon (Yaksajeon hall of Gwanyongsa temple), Changnyeong, Korea. *Journal of Conservation Science*. 2009;25:383-398.
3. Jeon YG, Lee CH. Pigment analysis for wall paintings according to verification of penetration depth for X-ray: Ssanggyesa Daeungjeon (main hall of Ssanggyesa temple) in Nonsan. *Journal of Conservation Science*. 2011;27:269-276.
4. Kim JS, Lee CH. Interpretation of coloring technique and pigment analysis for King Sejo's Palanquin in Gongju Magoksa temple, Korea. *Journal of Conservation Science*. 2019;35:403-415.
5. Jo YH, Lee CH. Making method of deterioration map and evaluation techniques of surface and three-dimensional deterioration rate for stone cultural heritage. *Journal of Conservation Science*. 2011;27:251-260.
6. Lee CH, Lee MS. The state of the art and conservation method for the masonry cultural heritages in Korea. *Journal of the Korea Institute for Structural Maintenance and Inspection*. 2005;9:13-21.
7. Gasanova S, Pagès-Camagna S, Andriotti M, Hermon, S. Non-destructive in situ analysis of polychromy on ancient Cypriot sculptures. *Journal of Archaeological and Anthropological Sciences*. 2016;10: 83–95.
8. Kogou S, Lucian A, Bellesia S, Burgio L, Bailey K, Brooks C, Liang H. A holistic multimodal approach to the non-invasive analysis of watercolour paintings. *Journal of Applied Physics*. 2015;121:999-1014.
9. Lia GH, Chen Y, Sun XJ, Duana PQ, Lei Y, Zhang An automatic hyperspectral scanning system for the technical investigations of Chinese scroll paintings. *Journal of Microchemical*. 2020;155:104699.
10. Liu ZF, Zhang H, Zhou WH, Hao SC, Zhou Z, Qi XK, Shi J. Pigment identification on an undated Chinese painting by non-destructive analysis. *Journal of Vibrational Spectroscopy*. 2019;101:28-33.
11. Tortora M, Sfarra S, Chiarini M, Daniele V, Taglieri G, Cerichelli G. Non-destructive and micro-invasive testing techniques for characterizing materials, structures and restoration problems in mural paintings. *Journal of Applied Surface Science*. 2016;387:971-985.
12. Wang J, Hao S, Zhou W, Qi X, Shi J. Research based on optical non-destructive testing of pigment identification. *Journal of Nanoscience and Nanotechnology*. 2016;16:3583-3586.
13. Zhongbin L, Wei W, Guohua S, Yuqing W, Julin W. Study on colored pattern pigments of a royal Taoist temple beside the Forbidden City (Beijing, China). *Journal of Vibrational Spectroscopy*. 2017;92:234-244.
14. Renate N. Cinnabar reviewed: characterization of the red pigment and its reactions. *Journal of Studies in Conservation*. 2015;60:79-87.
15. Lantes-Suarez O, Prieto B, Prieto-Martínez MP, Ferro-Vazquez C, Martínez-Cortizas A. The colour of ceramics from Bell Beaker contexts in NW Spain: relation to elemental composition and mineralogy. *Journal of Archaeological Science*. 2015;54:99-109.
16. McLellan MR, Lind LR, Kime RW. Hue angle determinations and statistical analysis for multi-quadrant Hunter L,a,b data. *Journal of Food Quality*. 1995;18:235-240.

Figures



Figure 1

The present status of the White-Robed Water-Moon Avalokiteshvara painting in this study. (A) Foreground of the painting. (B) Face part of the painting. (C) Nirmāna-Buddha on crown. (D) Left hand of the painting. (E) Bamboo in the upper right corner. (F) Seonjae Dongja (priestling) in the center right. (G) Kundika and willow branches in the middle left.

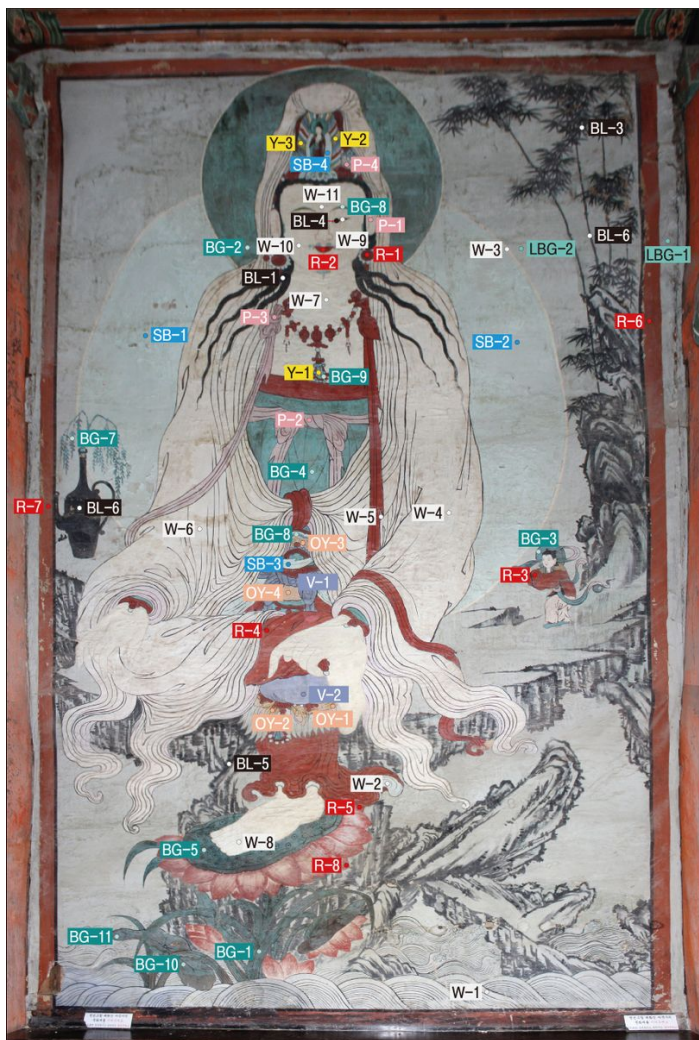


Figure 2

Photograph showing the detailed measurement points of P-XRF and chromaticity analysis in this study.



Figure 3

Photographs showing the representative damages of the studied painting. (A) Microcracks. (B) Separation. (C) Fragmentation. (D) Black contamination. (E) Blistering and exfoliation of the pigment layer. (F) Stereoscopic photographs of the exfoliation part on the pigment layers. (G) Deterioration of wooden frame after stripping the painting. (H) Residual pigments and cracks in the wooden frame.

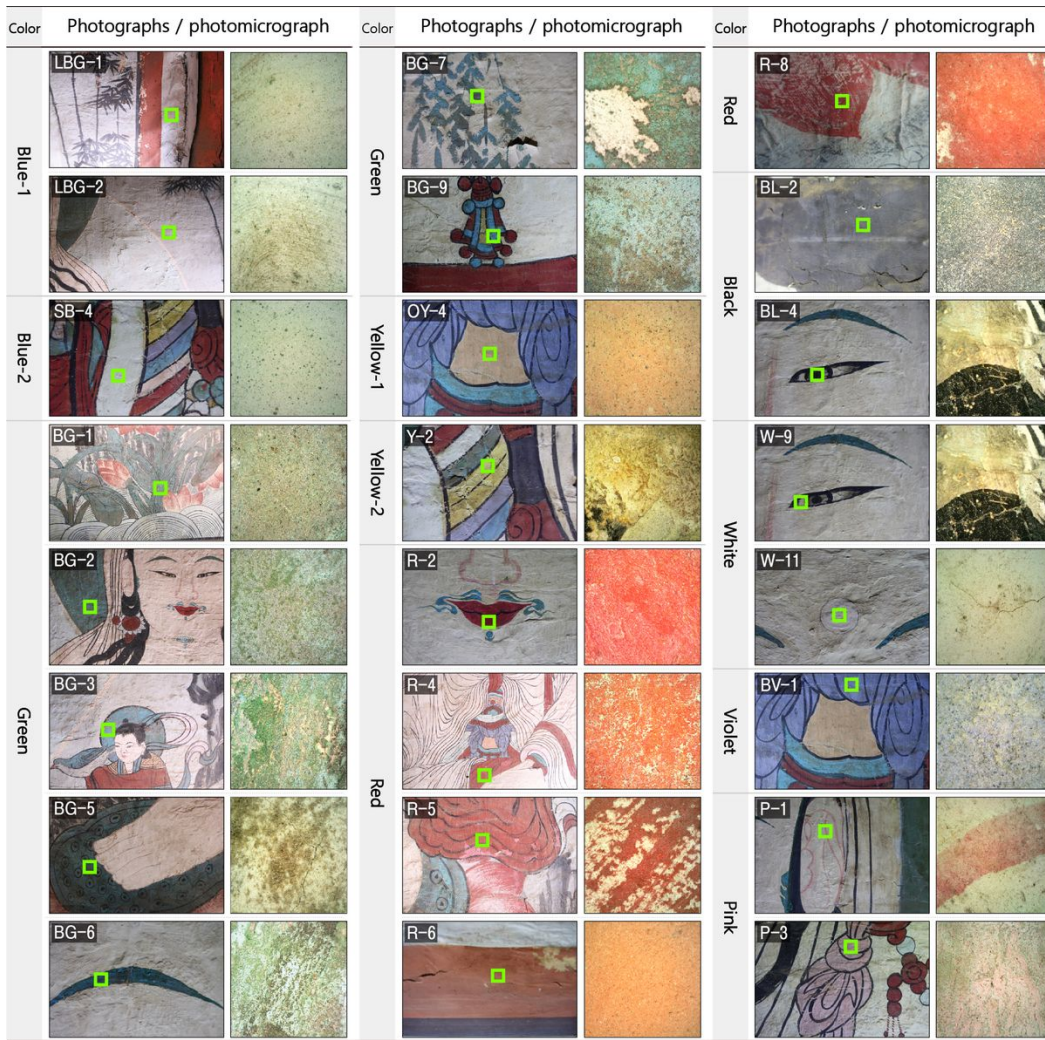


Figure 4

Photographs showing the measuring points and magnified images for pigment analysis in this study. Numbers are the same as those of Figure 2.

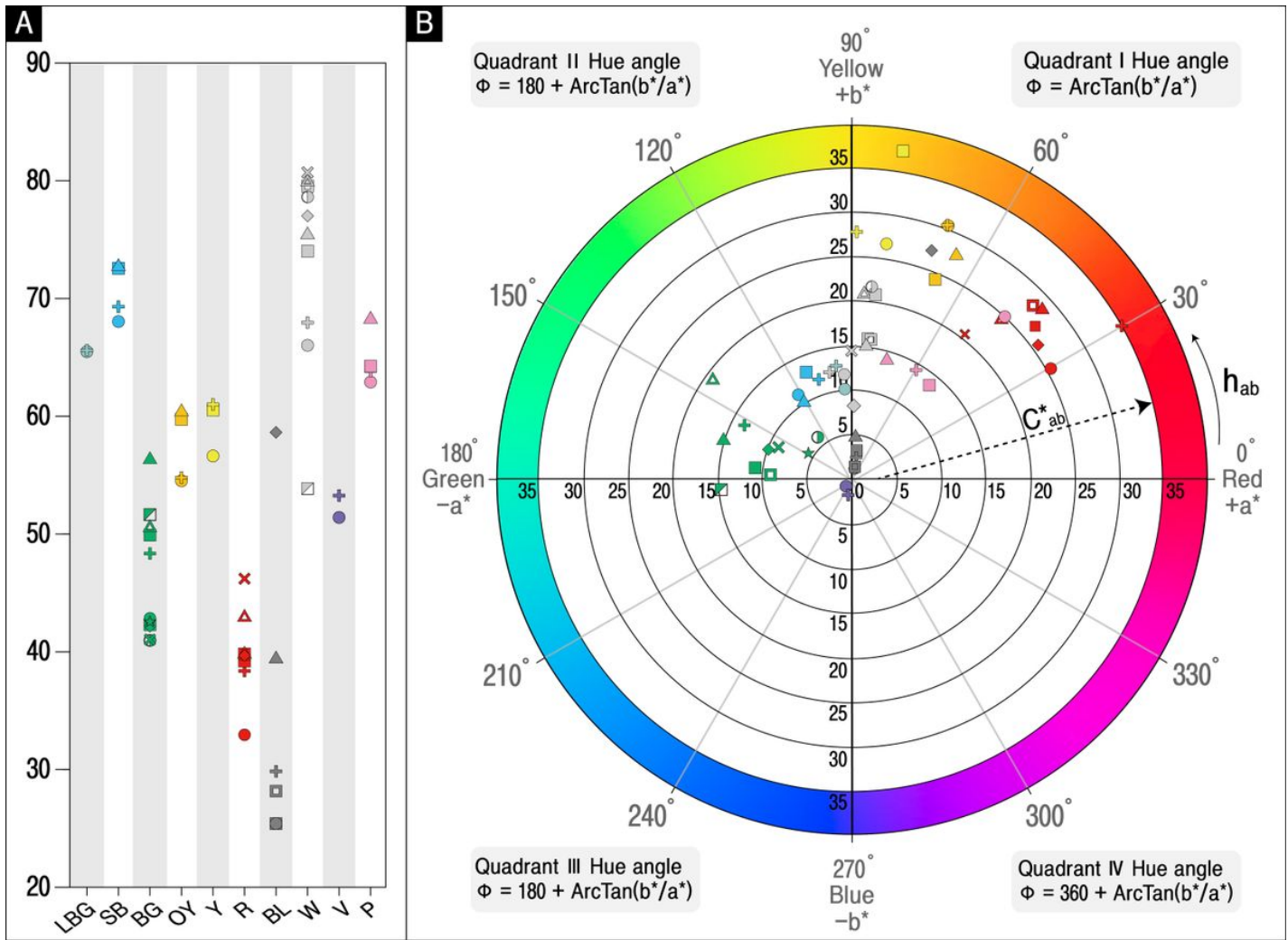


Figure 5

Diagrams showing the chromaticity analysis for coloring pigments in this study. (A) Luminosity. (B) Position of the analysis points projected in the a*-b* plane. The abbreviations are shown in Table 1 and the symbols are shown in Figure 6.

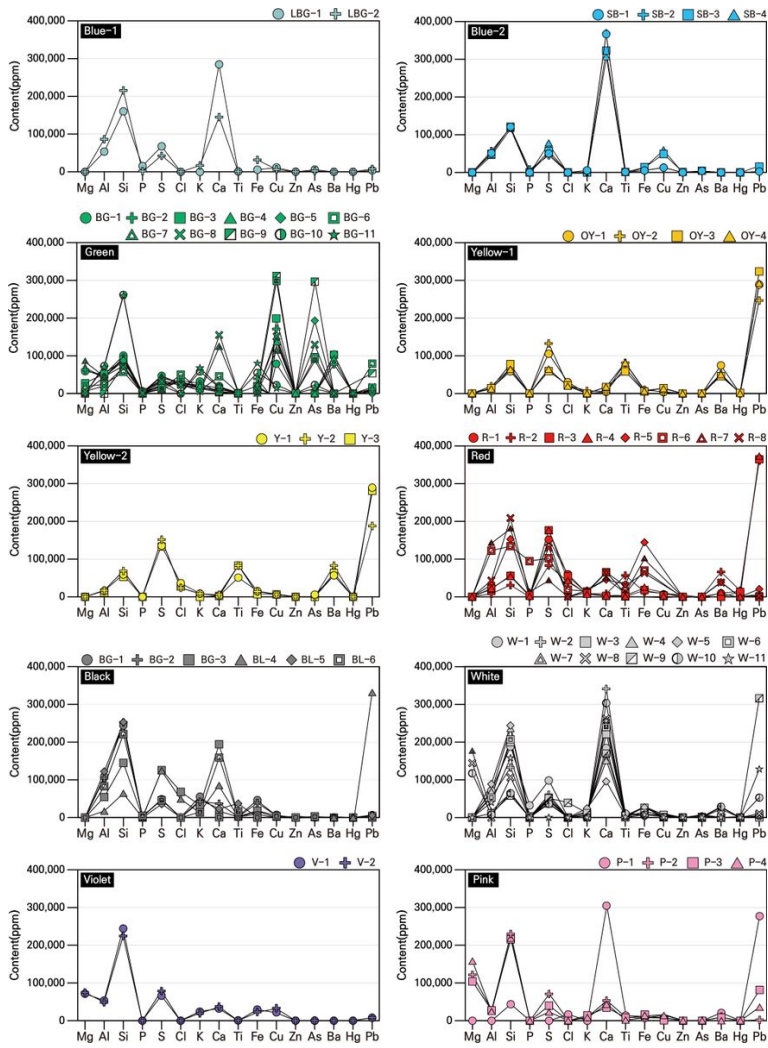


Figure 6

Diagrams showing the measurement results (ppm) of coloring pigments by P-XRF in this study. Numbers are the same as those of Figure 2.

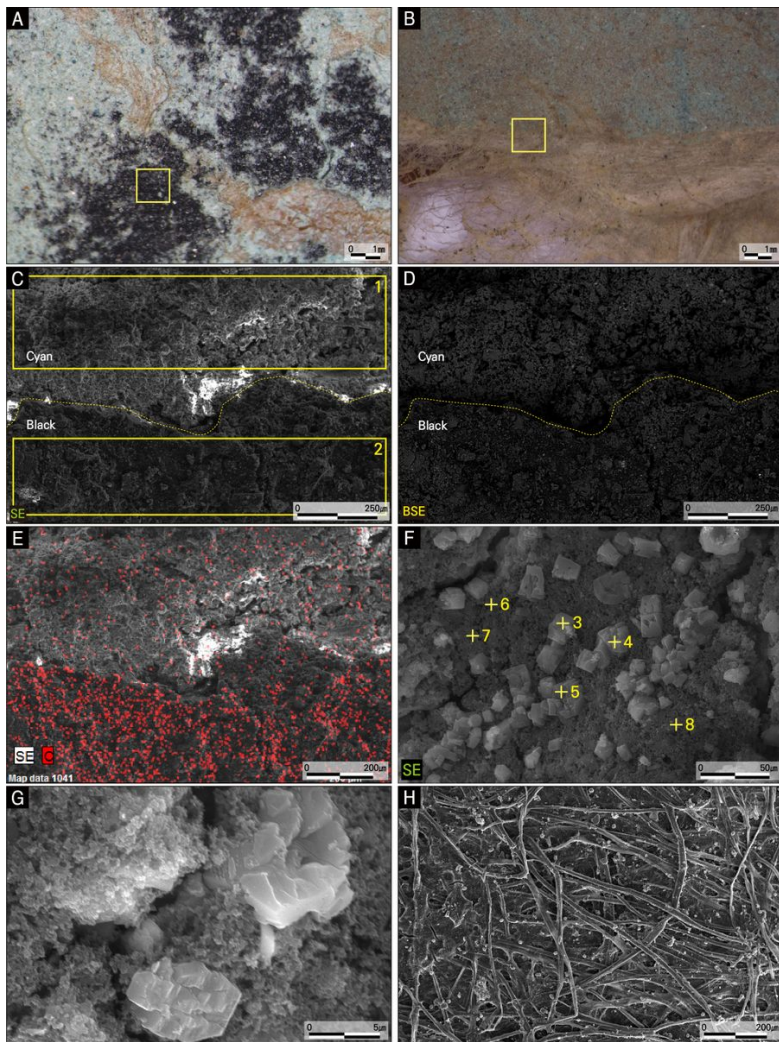


Figure 7
 Microphotograph images using optical microscope, SEM and EDS analytical spots for exfoliated black and cyan pigment samples in this study. (A, B) Occurrences under stereoscopic microscope at the analysis point. (C) SEM secondary electron image in Figure 3A. (D) SEM Back scattered electron image of Figure 3A. (E) Elemental mapping image using EDS analysis on the black and cyan layer. (F) SEM secondary electronic images of carbon particles in Figure 3A. (G) Enlarged particle image of Figure 3F. (H) SEM secondary electron image in Figure 3B.

Supplementary Files

This is a list of supplementary files associated with this preprint. Click to download.

- [TRANSLATIONCERTIFICATE.pdf](#)